Proc. Natl. Acad. Sci. USA
Vol. 92, pp. 6683–6688, July 1995
Colloquium Paper

This paper was presented at a colloquium entitled "Physics: The Opening to Complexity," organized by Philip W. Anderson, held June 26 and 27, 1994, at the National Academy of Sciences, in Irvine, CA.

Diffusion and formation of microtubule asters: Physical processes versus biochemical regulation

M. DOGTEROM, A. C. MAGGS*, AND S. LEIBLER

Departments of Physics and of Molecular Biology, Princeton University, Princeton, NJ 08544

ABSTRACT **Microtubule asters forming the mitotic spindle are assembled around two centrosomes through the process of dynamic instability in which microtubules alternate between growing and shrinking states. By modifying the dynamics of this assembly process, cell cycle enzymes, such as cdc2 cyclin kinases, regulate length distributions in the asters. It is believed that the same enzymes control the number of assembled microtubules by changing the "nucleating activity" of the centrosomes. Here we show that assembly of microtubule asters may be strongly altered by effects connected with diffusion of tubulin monomers. Theoretical analysis of a simple model describing assembly of microtubule asters clearly shows the existence of a region surrounding the centrosome depleted in GTP tubulin. The number of assembled microtubules may in some cases be limited by this depletion effect rather than by the number of available nucleation sites on the centrosome.**

A eukaryotic cell constructs a complex molecular machinery, called the mitotic spindle, in order to assure a precise division of its duplicated genetic material. The spindle consists mainly of long protein fibers, microtubules (MTs), assembled around two organizing centers, often called centrosomes. The MTs first attach to the duplicated chromosomes, order them in space, and then actively participate in their physical separation.

The assembly of the mitotic spindle is an example of a strongly regulated cellular process. An extended network of cell cycle enzymes is responsible for correct formation of the spindle, in synchrony with other cellular events. The interaction between these enzymes is mainly biochemical: they act on one another by introducing specific covalent modifications, such as phosphorylation or dephosphorylation. The cell cycle enzymes similarly modify the protein constituents of the mitotic spindle, in this way regulating its function.

To construct the mitotic spindle and to correctly separate the duplicated chromosomes, thousands of molecules have to move, to assemble into larger structures, to exert forces, etc. The underlying physical processes, such as directional movements, formation of physical connections, pushing, or pulling, are subject to thermal noise and often lack necessary precision. It is the role of biochemical regulation to assure that these physical processes "cooperate" with one another and lead to the functionally correct result: one copy of the genome in each daughter cell.

The interplay between physical and biochemical phenomena in the cell is often quite subtle and it is not easy to separate their effects. It is safe to say that for all functionally important tasks, of which the separation of the chromosomes is a good example, the cell uses mainly biochemical processes. They provide necessary feedbacks, checkpoints, and other regulation mechanisms. However, this does not mean that one can simply neglect the effects of the underlying physical phenomena. In what follows, we illustrate this point by considering an important event of the assembly of the mitotic spindle—the formation of MT asters around the two centrosomes.

Formation of Mitotic Microtubule Asters

At the entrance to mitosis, MT structures completely change their aspect. A nondividing (interphase) cell possesses a dense network of MTs extending from its nucleus to its periphery. At early stages of mitosis, this network is replaced by two dynamic "asters," which are MT structures organized radially around the centrosomes (17, 21, 22). The centrosomes separate in space and form two future poles of the mitotic spindle. However, before the spindle is fully formed the MTs have to "catch" the condensed chromosomes, which, after disassembly of the nucleus, are free to diffuse within the cell.

At the basis of aster formation and of the process of catching the chromosomes lies an assembly process of MTs called the dynamic instability (23). This phenomenon differs substantially from the reversible assembly of other polymers. It can be described, at the simplest level, as two distinct states of reversible polymerization, with infrequent random transitions between the states. In one of these states the polymer grows, in the other it shrinks; the transition from the growing to the shrinking state is called a catastrophe, the inverse transition is called a rescue. A MT can grow or shrink over distances of micrometers (thousands of monomers) before switching into the other state. Four dynamic parameters define this process: the growth velocity v_+, the shrinkage velocity v_-, and the transition rates f_{+-} (catastrophes) and f_{-+} (rescues). By analyzing stochastic equations describing the time evolution of each MT in this simple model, one can predict the existence of a sharp transition or a threshold between an unlimited or unbounded growth, with the average growth speed $J > 0$, and a steady-state or bounded growth, characterized by a well-defined MT steady-state length distribution with $J = 0$ (Fig. 1*B*). The transition can be reached by varying v_+, v_-, f_{+-}, or f_{-+} or simply by crossing some critical value of the monomer density $c = c_{cr}$.

The presence of the transition provides a very efficient mechanism for regulation of MT structures; by varying only slightly the effective parameters of the dynamic instability, the cell, or more precisely cell cycle enzymes, may change the distribution of polymer lengths. The relevance of such a mechanism for mitotic MTs has indeed been demonstrated in recent experiments with *Xenopus* egg extracts (1). They have demonstrated that the dynamic parameters measured in in-

The publication costs of this article were defrayed in part by page charge payment. This article must therefore be hereby marked "*advertisement*" in accordance with 18 U.S.C. §1734 solely to indicate this fact.

Abbreviation: MT, microtubule.

*On leave from: Laboratoire de Physico-Chimie Théorique, Ecole Supérieure de Physique et de Chimie Industrielles, 75231 Paris Cédex 05, France.

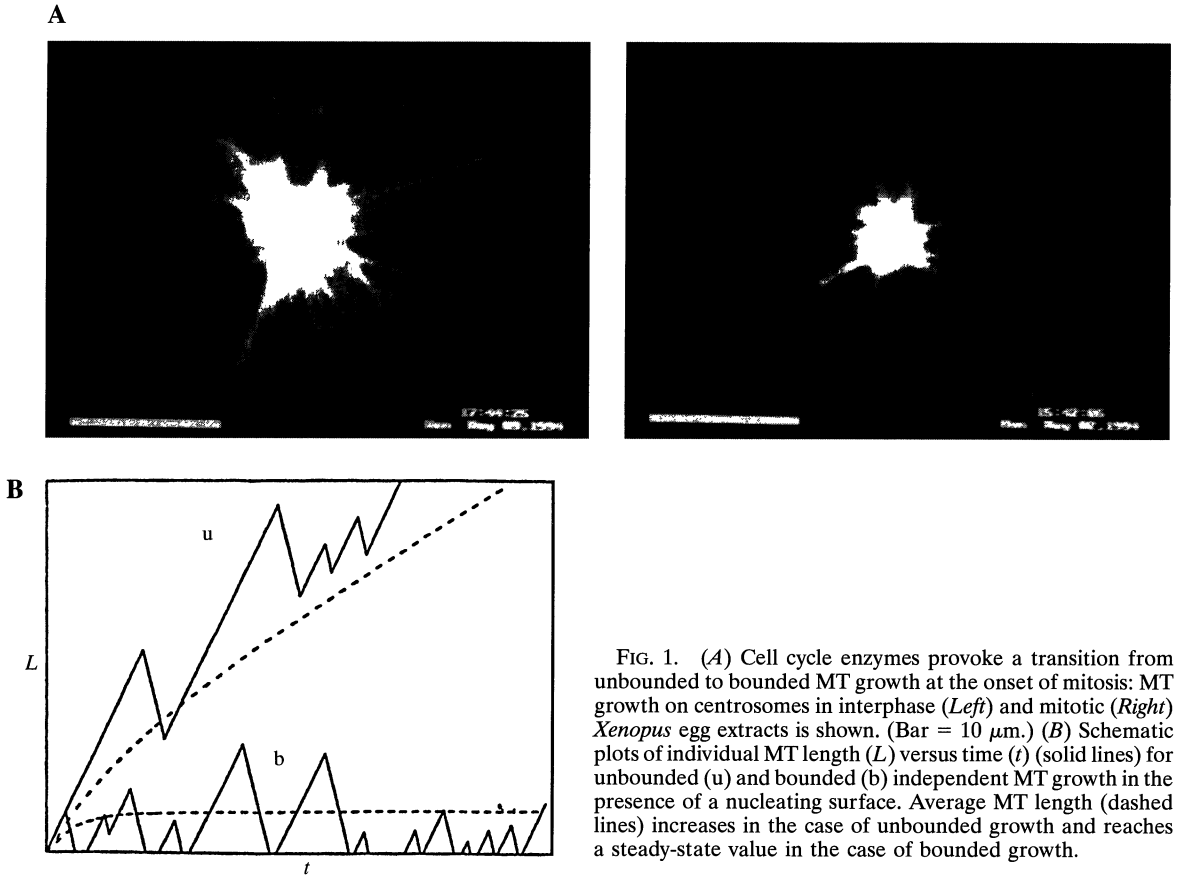

FIG. 1. (*A*) Cell cycle enzymes provoke a transition from unbounded to bounded MT growth at the onset of mitosis: MT growth on centrosomes in interphase (*Left*) and mitotic (*Right*) *Xenopus* egg extracts is shown. (Bar = 10 μm.) (*B*) Schematic plots of individual MT length (L) versus time (t) (solid lines) for unbounded (u) and bounded (b) independent MT growth in the presence of a nucleating surface. Average MT length (dashed lines) increases in the case of unbounded growth and reaches a steady-state value in the case of bounded growth.

terphase extracts are such that the MT system is in an unbounded growth state—i.e., growth of the aster is limited only by the total amount of tubulin or the size of the cell. In mitotic extracts, where two central cell cycle enzymes cdc2 cyclin A and cdc2 cyclin B kinases (24) are active, the asters are in the bounded growth state (Fig. 1*A*). The activity of cdc2 cyclin A kinase seems to modify all four dynamic parameters (1, 25, 26). Moderate changes are sufficient, however, to drive the system into the bounded growth state (with the average length of MTs of the order of 15 μm), because in the interphase extracts the system seems to be very close to the threshold (J positive but small). The activity of cdc2 cyclin B kinase, on the other hand, strongly increases the catastrophe frequency, f_{+-}. Consequently, the average length of the MTs decreases drastically (to about 3 μm).

Although the biochemical factor(s) responsible for this spectacular transformation—the substrate(s) of the kinase activity—still remains to be identified, it seems clear that at the entrance to mitosis the regulatory biochemical network acts by modifying the parameters of the dynamic instability, mainly the frequencies of catastrophes and rescues. In this way, it changes the morphology of structures formed by MTs. Instead of a dense network of fibers extending to the cortex of the cell (grown through an unbounded growth), the cell produces shorter, more dynamic asters (through a bounded growth), which are much more efficient for searching for the chromosomes. The fact that this change takes place through a transition process rather than through a gradual one is worth noting. More importantly, the very existence of this transition is a robust phenomenon: it does not depend on the details of the geometry or the exact growth dynamics. This robustness is crucial and is very general for biological systems.

Diffusion Effects

The simplest model of the dynamic instability assumes that MTs grow independently of each other and completely neglects "diffusion" effects—i.e., the possibility that MTs interact with each other through competition for incoming tubulin dimers. Diffusion effects have been a subject of intensive study for physical assembly processes such as crystal growth or small particle aggregation where they are often of crucial importance (2). However, relatively little effort has been made to study the role of diffusion for assembly of biological molecules such as actins or tubulins forming cytoskeletal fibers. The reason for this is that although the diffusion length l_D (3), which characterizes the range of depletion of the monomer pool, can be as big as 10–100 μm for a single growing MT, the amplitude of this perturbation decays quickly to relatively small values. Thus, for an isolated fiber it seems justified to neglect the depletion effects (4).

However, for a dense array of MTs assembled through the dynamic instability, the situation may be very different. For instance, one can show that for the MTs nucleated by a planar surface, the depletion region next to the surface controls the density of growing fibers (3). This happens even if the initial concentration of GTP-tubulin dimers c_T^0 is so high that the initially nucleated MTs are in a state of unbounded growth (1). The induced depletion of dimers near the surface alters the behavior of subsequently nucleated MTs, which are eventually trapped in a state of bounded growth (1). In consequence, the total number of MTs that manage to "escape" the surface is strongly dependent not only on c_T^0 or on the density of nucleation sites s_0 but also on the dimer diffusion constant D and the exact geometry of assembly.

One could try to extrapolate these results to the case of MTs nucleated from an organizing center such as a centrosome. They would mean that, in addition to biochemical regulation mechanisms such as biochemical controlling of the nucleation properties of the centrosome (5–8), the density of MTs would be strongly influenced by a purely physical effect of the diffusion of tubulin monomers.

To verify whether these diffusion effects may indeed be relevant for cellular assembly, we consider the case of MT asters nucleated radially from a centrosome (instead of the planar geometry considered before). We still make several simplifying assumptions by supposing MTs to be perfectly rigid, centrosomes to be spherical and isotropic, and that MTs lose dimers only from the distal, "plus" end [i.e., we neglect tubulin "flux" within the MTs (9)]. We are also obliged to neglect several plausible but until now little studied effects, such as a possible dependence of dynamic assembly parameters on the GDP-tubulin concentration or a possible formation of new nucleation centers with the increase of c_T. (Note, however, that this last effect would only reinforce the conclusions presented below.) On the other hand, our model takes into account many aspects completely neglected in the previous studies—namely (*i*) the diffusion of tubulin dimers; (*ii*) the dependence of the parameters of dynamic instability on local concentration of GTP-tubulin, c_T, as measured in recent experiments (10–12); (*iii*) the finite regeneration rate of GDP-tubulin into GTP-tubulin in the solution rich in free GTP (13); (*iv*) the finite density of nucleation sites s_0 for MTs on the centrosome (i.e., the fraction of its surface available for MT growth).

Solution of the Model

Mean-Field Theory. We use a set of four coupled mean-field equations, which neglect angular density fluctuations. They describe the time evolution of the length distributions of growing, $p_+(r,t)$, and shrinking, $p_-(r,t)$, MT tips, and the densities of both GTP-tubulin, $c_T(r,t)$, and GDP-tubulin, $c_D(r,t)$, dimers (r is defined as the distance to the center of the centrosome). The first two equations correspond to the process of dynamic instability; the other two describe the change in tubulin concentrations through (*i*) the exchange of dimers between MTs and free subunits; (*ii*) the regeneration of GTP-tubulin from GDP-tubulin (with the rate k); (*iii*) tubulin diffusion (with the diffusion constant D). The equations are

$$\partial_t p_+ = -f_{+-}p_+ + f_{-+}p_- - \partial_r(v_+p_+)$$

$$\partial_t p_- = +f_{+-}p_+ - f_{-+}p_- + v_-\partial_r p_-$$

$$\partial_t c_T = -v_+ s_0\left(\frac{R^2}{r^2}\right)p_+ + kc_D + D\nabla^2 c_T$$

$$\partial_t c_D = +v_- s_0\left(\frac{R^2}{r^2}\right)p_- - kc_D + D\nabla^2 c_D.$$

Here R is the radius of the centrosome, and the microscopic length scale (the size of a protein) is set to 1. These equations are solved by standard numerical techniques, consisting of a mixture of implicit and explicit discretization schemes to solve partial differential equations, with the following boundary conditions: $c_T|_{r=\infty} = c_T^0$; $\partial_r c_T|_{r=R} = 0$; $\partial_t c_D|_{r=R} = 0$; $u_+p_+|_{r=R} = \tau s/s_0$; $\partial_t s = -v_+p_+s_0|_{r=R} + v_-p_-s_0|_{r=R}$. Here s (as opposed to s_0) is the density of free nucleation sites and $\tau c_T|_{r=R}$ is the nucleation rate (for simplicity we assume a first-order nucleation process). The results are used to obtain the values for ρ, the surface density of MTs. At any time, the surface density of MTs is given by the product of the density of nucleation sites and the probability that a given site is occupied by a MT of nonzero length:

$$\rho = s_0\int_0^\infty [p_+(r) + p_-(r)]dr.$$

To compare the results with the case of independent MT growth (neglecting diffusion effects), we solved numerically the corresponding mean-field equations. They are identical to the first two of the above equations, with $c_T = c_T^0$ for all r and t.

The values of the parameters are chosen in the following way: (*i*) At $c_T = 10$ μM they are set to correspond to typical values found in interphasic cellular extracts for individual MTs (1): $v_+ \cong 10$ μm/min; $v_- \cong 15$ μm/min; $f_{+-} \cong 0.012$ s^{-1}; $f_{-+} \cong 0.02$ s^{-1}. (*ii*) Since this set of values corresponds to a near-threshold situation, by varying c_T we can then easily explore diffusion effects both below and above the critical concentration. We obtain the values of the dynamic parameters at other GTP-tubulin concentrations by assuming the following phenomenological c_T dependencies based on recent experimental data (10–12): $v_+ \equiv u_+c_T$, with u_+ independent of c_T; v_- = constant; $f_{-+} \equiv \omega c_T$, where ω is a constant; f_{+-} strongly decreasing with increasing c_T.

We chose a particular functional form of this last dependence that fits well the available experimental data on catastrophe rates in pure tubulin solutions (H. Flyvbjerg, T. E. Holy, and S.L., unpublished data). It results from the analysis of a recent phenomenological model of the catastrophes in dynamic instability. This model assumes that a MT has at its tip a stabilizing "cap"; a catastrophe takes place when this cap disappears. The stabilizing cap grows by addition of new GTP-tubulin dimers and shrinks with a constant rate at its other end due to a progressive, induced hydrolysis of the GTP nucleotides and/or a conformational change of tubulin. In addition, the cap can decrease in size at any time by a random "spontaneous event" of hydrolysis and/or of conformational change taking place along its whole length. How often the size of this cap shrinks to zero, and in consequence a catastrophe

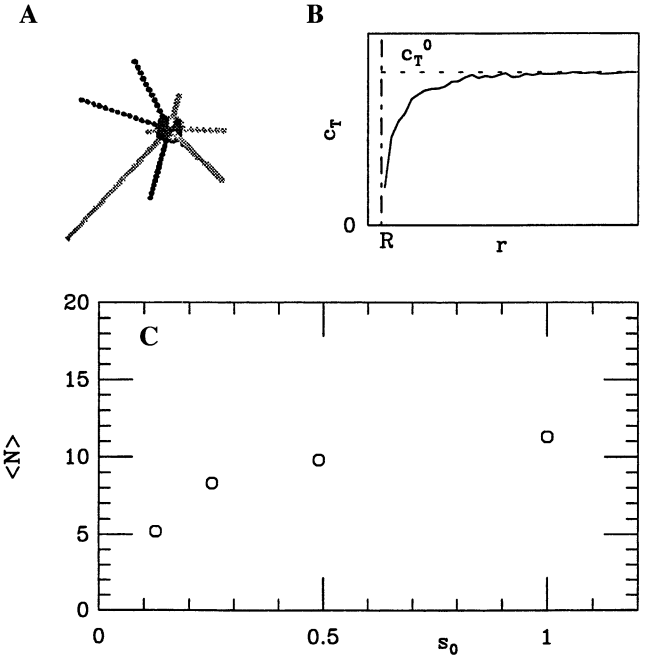

FIG. 2. (*A*) MT aster in a state of bounded growth (obtained through three-dimensional Monte Carlo simulations), showing the geometry for MT assembly and tubulin diffusion. We consider isotropic growth of perfectly rigid MTs nucleated from a spherical centrosome with radius R. (*B*) Corresponding steady-state GTP-tubulin profile c_T in the region surrounding the centrosome, showing depletion due to the assembly of MTs. c_T^0 is the initial concentration of GTP-tubulin dimers. (*C*) Average number of nucleated MTs as a function of s_0, where $0 \leq s_0 \leq 1$ is the total surface density of nucleation sites (i.e., fraction of the centrosome area capable of MT nucleation). For small s_0, the number of MTs growing out of the centrosome is limited by the number of available nucleation sites ("site-limited" regime), while for large s_0 it is limited by diffusion effects ("diffusion-limited" regime); see Fig. 4 and text.

event occurs, depends in this model on only two parameters: v_{AB}, the average induced shrinkage velocity of the cap; and r, the rate of spontaneous events per unit length of the cap. We chose these two parameters to fit the desired catastrophe rate at $c_T = 10\ \mu M$. The results of our calculation are shown for $v_{AB} = 6\ \mu m/min$ and $r = 655\ min^{-1}/\mu m$, but similar results were obtained for $v_{AB} = 4\ \mu m/min$ ($r = 1076\ min^{-1}/\mu m$) and $v_{AB} = 2\ \mu m/min$ ($r = 1632\ min^{-1}/\mu m$) (data not shown). The choice of a particular functional form of the c_T dependence of the catastrophes does not seem crucial; similar results were also obtained when we assumed a simple exponential dependence: $f_{+-} \equiv Ae^{-\sigma c_T}$, where we varied the value of σ between 0.2 and 0.5 μM^{-1} (data not shown). Other values used are $R = 1\ \mu m$; $D = 5\ \mu m^2/s$ (14); $k = 0.02\ s^{-1}$ (13); $\tau = 0.15\ \mu M^{-1}/min$.

Monte Carlo Simulations. As well as solving the mean-field equations, we performed three-dimensional Monte Carlo simulations in order to verify that angular density fluctuations do not significantly change the results. In these "off-lattice" simulations a MT-nucleating spherical object (a centrosome) is centered in a spherical container filled with diffusing subunits. A MT nucleates whenever a GTP-tubulin subunit moves close enough to the nucleating sphere, and a MT grows whenever such a subunit moves close enough to a growing MT tip. Growing MTs convert to shrinking MTs with some constant probability. Shrinking MTs lose subunits from their tip at a constant rate; these disassembled GDP-tubulin subunits cannot directly stick to growing MT tips but have first to convert back, at a constant rate, to GTP-tubulin subunits. Rescues occur when GTP-tubulin subunits adhere—with a low probability—to shrinking MTs. Catastrophes occur when a MT cap disappears according to the rules given by the model described above. We vary the total amount of nucleating sites—i.e., the total surface available for nucleation, s_0—by dividing the nucleating surface into a constant number of patches of variable size and allowing MTs to be nucleated only when GTP-tubulin subunits move close enough to these patches. The parameters are chosen to obtain a MT population in a state of bounded growth (they roughly mimic typical values found in mitotic cellular extracts). The average number of nucleated MTs as well as the radial distribution of GTP-tubulin subunits are studied after the MT population reaches its steady state.

Results

An example of MTs (in a state of bounded growth) nucleated at a spherical centrosome in our Monte Carlo simulations is shown in Fig. 2*A*. A typical GTP-tubulin profile for this geometry is depicted in Fig. 2*B*. Similar curves have been obtained by numerically solving the mean-field equations, where one neglects the angular dependence of density fluctuations. It is clear from these curves that a depletion region forms next to the nucleating surface in a steady state and that

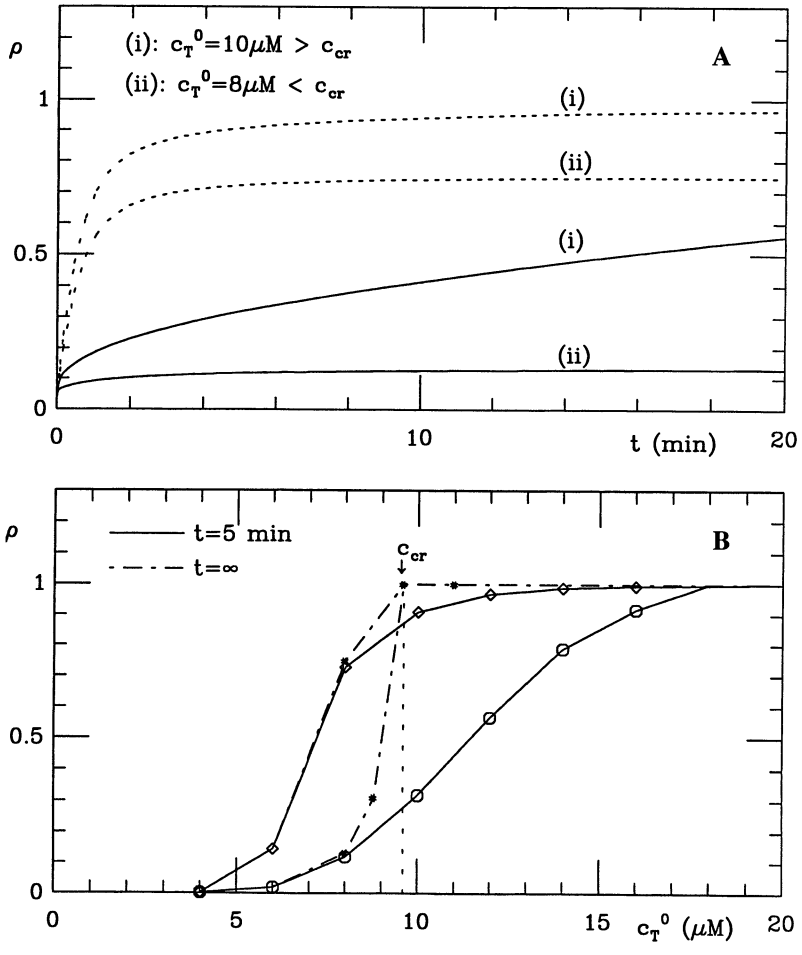

FIG. 3. (*A*) Mean-field results for time evolution of the density of MTs, ρ, on the surface of the centrosome (i.e., fraction of the centrosome area that is covered by MTs) for two different values of initial GTP-tubulin concentration c_T^0: one above (*i*) and one below (*ii*) the critical concentration for unbounded growth (c_{cr}; see text). We compare the case in which diffusion effects are included (solid curves) with the situation in which they are completely neglected (dashed curves). (*B*) ρ, as a function of initial bulk GTP-tubulin concentration c_T^0. Symbols (connected by solid lines) show densities at a finite time typical for experiments (5 min) both including (○) and neglecting (◇) diffusion effects. Dashed lines indicate these densities extrapolated to the infinite time limit.

it affects strongly the assembly (e.g., the average number, $\langle N \rangle$, of assembled MTs shown in Fig. 2*C*; see below).

Fig. 3*A* shows mean-field results for the time evolution of the density ρ of MTs nucleated by a centrosome—i.e., the fraction of the spherical surface from which MTs are actually growing. We depict here the solutions for two different values of the initial concentration c_T^0, one above and one below the threshold concentration c_{cr}. To reveal the role played by diffusion effects, we also plot the time evolution of the density of independent MTs, for which one neglects any spatial variation of the tubulin concentration c_T.

Below the threshold, the density of MTs rapidly settles at some steady-state value smaller than the one corresponding to the maximal coverage of the centrosome. This happens even in the case of independent growth; however, the asymptotic value is markedly decreased by the diffusion effects: it takes a relatively long time for "fresh" GTP-tubulin to diffuse into the depleted region or for GDP-tubulin to regenerate back to the GTP form. Above the threshold concentration c_{cr}, the density of MTs quickly converges to the complete coverage for independent growth, while in the presence of tubulin depletion the convergence is very slow; when observed on experimental time scales (5–20 min), the density of MTs may even give the impression of "saturating" at some level below the maximum (especially for a finite resolution of experimental measurements of ρ; see ref. 5).

This finite time effect is also emphasized in Fig. 3*B*, which shows the dependence of the MT density on the initial concentration c_T^0. Again, by comparing the solutions of diffusion equations with the case of independent MTs, we see—for the typical times of experiments—that the density of MTs is limited by diffusion effects for concentrations well above the threshold concentration c_{cr}, while in the infinite time limit (obtained through an appropriate extrapolation) this is only the case below c_{cr}.

It is worth noting that the general aspect of these curves closely agrees with the experimental data reported for MT asters growing in pure tubulin solutions (5, 15). More quantitative experiments in tubulin solutions or cell extracts should allow for a detailed comparison with the predictions of our calculations.

Conclusions: Biochemical Regulation Versus Diffusion Effects

Although the results presented in Fig. 3 clearly show that the diffusion strongly influences the assembly of dense MT systems (as opposed to isolated MTs), one could still argue that such diffusion effects can be neglected compared with the biochemical regulation mechanisms. As discussed in *Formation of Mitotic Microtubule Asters*, biochemical mechanisms are important in regulation of the length distribution of assembled MTs: during the transition from interphase to mitosis the active kinases transform long MTs into shorter and more dynamic ones by changing the parameters of dynamic instability (1). Similarly, the cdc2 cyclin kinases could control the number of MTs by increasing nucleating activity of the centrosomes. The simplest way in which this might happen is through changes in the number of active nucleation sites, either through assembly of new nucleating complexes [built with γ-tubulin (16) and associated proteins (17, 18)] or through activation of some preexisting sites. To try to compare the

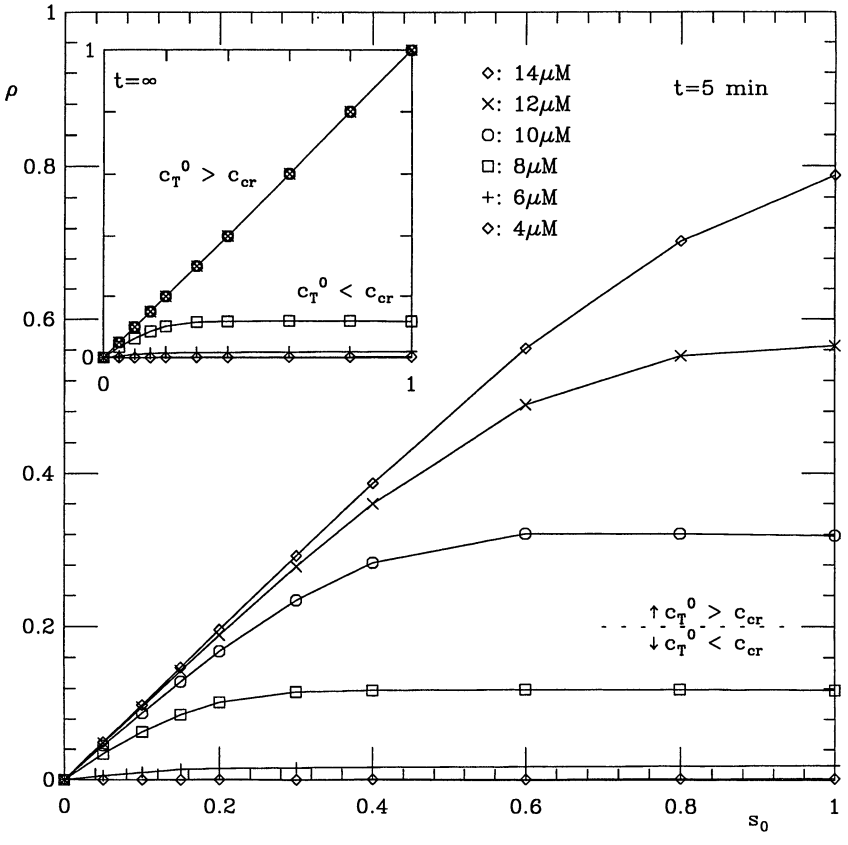

FIG. 4. Mean-field results for surface density of MTs, ρ, at experimental time scales (5 min) as a function of total density of nucleation sites s_0 for different values of initial GTP-tubulin concentration. (*Inset*) Same plots in the infinite time limit. In the case of independent growth, one expects the density of MTs to be site-limited and to increase linearly with the available density of nucleation sites. However, these curves clearly show that in the presence of diffusion a crossover exists from a site-limited density of MTs to a diffusion-limited regime, where the density of MTs is almost independent of the density of nucleation sites. For finite times, this crossover exists for values of c_T^0 both above and below the critical concentration for unbounded growth, while in the infinite time limit it exists only below the threshold.

relative importance of diffusive and biochemical effects, we have thus varied the density of nucleation sites s_0 on the centrosome. Using the mean-field theory, we find (Fig. 4) that in general there exist two regimes of aster behavior: (*i*) for small s_0 a "site-limited" regime in which the MT number is solely determined by the number of active sites; (*ii*) for larger s_0 a "diffusion-limited" regime in which the number of MTs growing out of the centrosome is smaller than and almost independent of the number permitted by active nucleation sites. (In infinite time limits this last regime is present only for c_T^0 smaller than the threshold value c_{cr}, but for typical time scales of cellular events or *in vitro* experiments both regimes exist for all c_T^0.) The existence of a crossover between these two regimes is also confirmed in three-dimensional simulations. In Fig. 2*C*, we plot the average number of nucleated MTs for four different values of s_0 for the case of bounded MT growth. We find that this number does not increase linearly with s_0 as expected in the absence of diffusion effects, but instead it levels off to a near-constant value.

An important point is that for realistic values of dynamic parameters and tubulin concentrations this crossover can happen for very small values of the surface MT density ρ. The crossover values of ρ being of the order of 0.01 (typical for lower curves in Fig. 4) correspond to roughly a hundred MTs [estimated as $(R/d)^2\rho$, where R is the centrosome radius, while d is the MT cross-section radius]. Therefore, for the MT asters that contain more than 10–1000 MTs, it is safe to say that the diffusion effects may not *a priori* be neglected and in fact in many cases they may be dominant. Fig. 4 suggests also a conceptually simple way of distinguishing between the site-limited and diffusion-limited regimes. By progressively blocking the nucleation sites and thus decreasing s_0—e.g., through the use of appropriate antibodies (19, 20)—one would linearly decrease the number of nucleated MTs only in the site-limited regime; in contrast, in the diffusion-limited regime the number of nucleated MTs would stay practically constant.

Obviously, our mathematical model cannot demonstrate that it is the diffusion effects, and in particular the tubulin depletion near the centrosome, that determine the number of MTs growing in an aster or a mitotic spindle. However, it shows that even in the presence of strong biochemical regulation the diffusion-induced effects may play an important role in the assembly of cytoskeletal fibers, as they do in many simpler physical systems. Therefore, while studying the biochemistry and the cell biology of the centrosomes and their regulation during the cell cycle, one must also keep in mind the underlying physical phenomena.

We would like to thank E. Karsenti, T. Holy, M. A. Félix, D. A. Huse, and B. Alberts for useful discussions and comments. This work was partially supported by the National Science Foundation (Grant PHY-9408905) and the National Institutes of Health (Grant GM50712).

1. Verde, F., Dogterom, M., Stelzer, E., Karsenti, E. & Leibler, S. (1992) *J. Cell Biol.* **118,** 1097–1108.
2. Vicsek, T. (1992) *Fractal Growth Phenomena* (World Scientific, Singapore).
3. Dogterom, M. & Leibler, S. (1993) *Phys. Rev. Lett.* **70,** 1347–1350.
4. Bayley, P. (1993) *Nature (London)* **363,** 309 (lett.).
5. Buendia, B., Draetta, G. & Karsenti, E. (1992) *J. Cell Biol.* **116,** 1431–1442.
6. Masuda, H., Sevik, M. & Cande, W. Z. (1992) *J. Cell Biol.* **117,** 1055–1066.
7. Ohta, K., Shiina, N., Okumura, E., Hisanaga, S.-I., Kishimoto, T., Endo, S., Gotoh, Y., Nishida, E. & Sakai, H. (1993) *J. Cell Sci.* **104,** 125–137.
8. Bré, M. H. & Karsenti, E. (1990) *Cell Motil.* **15,** 88–98.
9. Mitchison, T. J. & Sawin, K. E. (1990) *Cell Motil. Cytoskel.* **16,** 93–98.
10. Walker, R. A., O'Brien, E. T., Pryer, N. K., Sobeiro, M. F., Voter, W. A., Erickson, H. P. & Salmon, E. D. (1988) *J. Cell Biol.* **107,** 1437–1448.
11. Walker, R. A., Pryer, N. K. & Salmon, E. D. (1991) *J. Cell Biol.* **114,** 73–81.
12. Drechsel, D. N., Hyman, A. A., Cobb, M. H. & Kirschner, M. W. (1992) *Mol. Biol. Cell* **3,** 1141–1154.
13. Melki, R., Carlier, M.-F. & Pantaloni, D. (1988) *EMBO J.* **7,** 2653–2659.
14. Salmon, E. D., Saxton, W. M., Leslie, R. J., Karow, M. L. & McIntosh, J. R. (1984) *J. Cell Biol.* **99,** 2157–2164.
15. Mitchison, T. & Kirschner, M. (1984) *Nature (London)* **312,** 232–237.
16. Oakley, B. R. (1992) *Trends Cell Biol.* **2,** 1–5.
17. Kalt, A. & Schliwa, M. (1993) *Trends Cell Biol.* **3,** 118–128.
18. Raff, J. W., Kellogg, D. R. & Alberts, B. M. (1993) *J. Cell Biol.* **121,** 823–835.
19. Joshi, H. C., Palacios, M. J., McNamara, L. & Cleveland, D. W. (1992) *Nature (London)* **356,** 80–83.
20. Moudjou, M., Paintrand, M., Vigues, B. & Bornens, M. (1991) *J. Cell Biol.* **115,** 129–140.
21. Bornens, M. (1992) in *The Centrosome*, ed. Kalnins, V. I. (Academic, San Diego), pp. 1–44.
22. Kellogg, D. R., Sullivan, W., Theurkauf, W., Oegema, K., Raff, J. W. & Alberts, B. M. (1991) in *The Cell Cycle*, Cold Spring Harbor Symposia on Quantitative Biology (Cold Spring Harbor Lab. Press, Plainview, NY), Vol. 56, pp. 649–662.
23. Mitchison, T. & Kirschner, M. (1984) *Nature (London)* **312,** 237–242.
24. Nigg, E. A. (1993) *Trends Cell Biol.* **3,** 296–301.
25. Belmont, L. D., Hyman, A. A., Sawin, K. E. & Mitchison, T. J. (1990) *Cell* **62,** 579–589.
26. Verde, F., Labbé, J. C., Dorée, M. & Karsenti, E. (1990) *Nature (London)* **343,** 233–238.